

Supplementary Information for:

INCLINATION OF POLARIZED ILLUMINATION INCREASES SYMMETRY
OF STRUCTURES GROWN VIA INORGANIC PHOTOTROPISM

MADLINE C. MEIER,^a NATHAN S. LEWIS,^{*ab} AZHAR I. CARIM^{*ab}

^aDivision of Chemistry and Chemical Engineering

^bBeckman Institute

California Institute of Technology

Pasadena, CA 91125

*E-mail: nslewis@caltech.edu, aic@caltech.edu

S1. Contents

This document contains a description of the experimental and modeling/simulation methods utilized in this work (Sections S2 and S3), Fourier spectra fit data (Section S4), and a list of associated references (Section S5).

S2. Experimental Methods

Materials and Chemicals H₂SO₄ (ACS Reagent, J. T. Baker), buffered HF improved etchant (Transene), SeO₂ (99.4 %, Alfa Aesar), and TeO₂ (99+ %, Sigma-Aldrich) were used as received. H₂O with a resistivity ≥ 18.2 M Ω cm (Barnstead Nanopure System) was used throughout. Au-coated n⁺-Si(100) (< 0.005 Ω cm, As-doped, 525 ± 25 μ m thick, single-side polished, Addison Engineering) was used as a substrate for deposition. Flash-Dry Ag Paint (SPI Supplies), EP21ARHTND Epoxy (MasterBond) and nitrocellulose-based nail polish were used to assemble the working electrodes.

Substrate Preparation n⁺-Si wafers were etched with buffered HF for 30 s, rinsed with H₂O, dried under a stream of N₂(g), and then immediately transferred to an electron-beam metal evaporator with a base pressure $< 10^{-6}$ torr. Using an accelerating voltage of 10 kV, a 10 nm Ti adhesion layer was deposited on the polished side of the wafer using a 40 mA deposition current, and 50 nm of Au was then deposited on top of the Ti using a 150 mA deposition current. 20 nm of Ti was deposited on the unpolished side of the wafer to serve as a back-contact. The Au-topped Si sections were then cut into square 0.50 cm by 0.50 cm sections for use as deposition substrates.

Electrode Preparation Electrode assemblies were prepared by applying epoxy to the flat sides of each of two Al half-round bars (0.25 in diameter). The two bars were then joined together, with an ~ 10 mm offset in the axial dimension to form a cylinder with two half-round ends. Polytetrafluoroethylene heat-shrink tubing was used to insulate the cylindrical section and epoxy was used to insulate the rounded side of one of the half-round ends. Ag paint was applied to the Ti-coated back surfaces of the Au-topped Si sections and the sections were affixed to the flat surface of the epoxied half-round end. Nail polish was used to insulate the remaining uncovered area on the flat surface that surrounded the Au-topped Si section. Figure S1 presents a schematic

of an electrode assembly with an attached Au-topped Si section. Immediately before deposition, the surface of each electrode was briefly cleaned using a stream of $N_2(g)$.

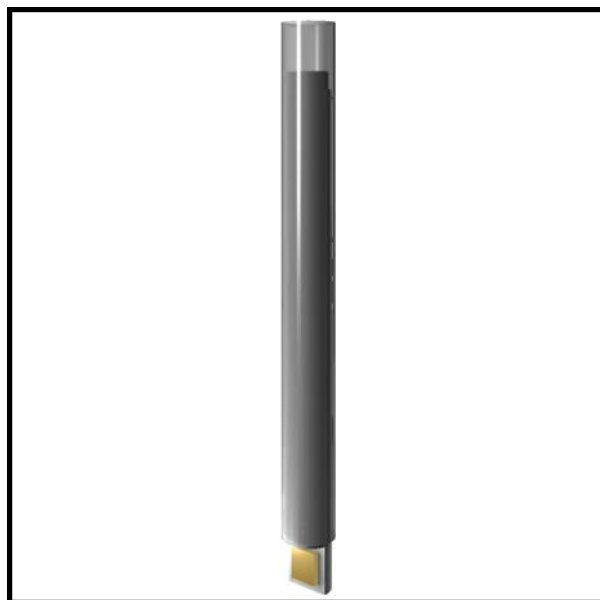


Figure S1. Schematic of an electrode assembly with an attached Au-topped Si section.

Electrode Illumination Illumination for photoelectrochemical growth was generated using a narrowband diode (LED) source with an intensity-weighted average wavelength, λ_{avg} , value of 626 nm and a spectral bandwidth (FWHM) of 17 nm (Thorlabs, SOLIS-623C). The LED output was collected, condensed and collimated using an aspheric lens ($\text{\O}25.4$ mm, $f = 16$ mm) followed by a bi-convex lenses ($\text{\O}50.8$ mm, $f = 60$ mm) and another aspheric lens ($\text{\O}50.8$ mm, $f = 32$ mm). A broadband film polarizer (LPNIRE200-B) was inserted before the final lens to effect linear polarization. A 1500 grit ground-glass (UV Fused Silica) diffuser was placed immediately in front of the photoelectrochemical cell to ensure spatial homogeneity of the illumination. The light intensity incident on the electrode was measured by placing a calibrated Si photodiode (Thorlabs FDS100), instead of an electrode assembly, in the photoelectrochemical cell with electrolyte, and the steady-state current response of that Si photodiode was measured. Depositions with normally-incident illumination were performed with a light intensity of $I = 30 \text{ mW cm}^{-2}$. For depositions

with off-normal incidence, the illumination was inclined from the substrate normal in the plane of the polarization by an angle β , and the intensities were increased by a factor of $\cos^{-1}(\beta)$ relative to the intensities used at normal incidence.

Photoelectrochemical Deposition Photoelectrochemical deposition was performed using a Bio-Logic SP-200 potentiostat. Deposition was performed in a two-compartment glass cell with a quartz window. A three-electrode configuration was utilized with an Ir wire counter electrode (99.999 %, Sigma-Aldrich) isolated behind a porous glass frit and a Ag/AgCl reference electrode (3.00 M KCl, Bioanalytical Systems). Films were deposited from an aqueous solution of 0.0200 M SeO₂, 0.0100 M TeO₂, and 2.00 M H₂SO₄. Photoelectrodeposition on isotropic substrates was effected by biasing the Au-coated electrode, illuminated as detailed under the above subheading (Electrode Illumination), potentiostatically at -0.15 V vs. Ag/AgCl for 4.00 min at room temperature. After deposition, the electrode was immediately removed from the cell, rinsed with H₂O, and then dried under a stream of N₂(g). The Au-coated substrate with top-facing Se-Te film was mechanically separated from the rest of the electrode assembly. The nitrocellulose-based insulation and the majority of the Ag paint were then removed mechanically.

Microscopy Scanning-electron micrographs (SEMs) were obtained with a FEI Nova NanoSEM 450 at an accelerating voltage of 5.00 kV with a working distance of 5.0 mm and an in-lens secondary electron detector. Micrographs obtained for quantitative analysis were acquired with a resolution of 172 pixels μm^{-1} over $\sim 120 \mu\text{m}^2$ areas. Micrographs that were used to produce display figures were acquired with a resolution of 344 pixels μm^{-1} over $\sim 2 \mu\text{m}^2$ areas.

S3. Modeling and Simulation Methods

Simulation of Deposit Morphology Light-directed electrochemical growth was simulated with an iterative growth model in which electromagnetic simulations were first used to calculate the local light absorption profile at the growth interface. Then, mass addition was simulated via a Monte Carlo method wherein the local absorption weighted the local rate of mass addition along the film surface.

Three-dimensional simulations were discretized using a cubic mesh with a lattice constant of 10 nm. Growth began with a bare, semi-infinite planar substrate. In the first step, the light-absorption profile under a linearly polarized, plane-wave illumination source with $\lambda_{\text{avg}} = 626$ nm was calculated using full-wave finite-difference time-domain (FDTD) simulations (“FDTD Solutions” software package, Lumerical). Perfectly matched layer boundary conditions were used in the direction normal to the substrate. For simulations using normally incident illumination, periodic boundary conditions were used for the two orthogonal directions in the plane of the substrate. For simulations using inclined illumination, periodic and Bloch boundary conditions were used in the directions in the plane of the substrate orthogonal to, and parallel to, the plane of illumination inclination, respectively. Previously measured values of the wavelength-dependent complex refractive index of Se-Te were used, and a value of $n = 1.33$ was used as the refractive index of the electrolyte.¹

In the second step, a Monte Carlo simulation was performed in which an amount of mass, equaling that of a 15 nm planar layer covering the simulation area, was added to the upper surface of the structure with a probability F :

$$F(A) = A \prod_{i=1}^3 \frac{x_i}{r_i} \text{ (Equation 1)}$$

where A is the spatially dependent absorption at the deposit/solution interface, x_i is the fraction of

i^{th} nearest neighbors occupied in the cubic lattice, and r_i is the distance to the i^{th} nearest neighbor. The multiplicative sum in the definition of this probability (Equation 1) serves to reduce the surface roughness of the film to mimic the experimentally observed surface roughness.

After the initial Monte Carlo simulation, the absorption of the new, structured film was then calculated in the same manner as for the initial planar film, and an additional Monte Carlo simulation of mass addition was performed. This process of absorbance calculation and mass addition was repeated until the simulated morphologies had heights equivalent to those exhibited by the experimentally generated deposits.

Dipole Simulations FDTD simulations of dipole emission were used to model the effect of illumination inclination on the optical field profile generated by light scattering at the growth interface. A two-dimensional simulation plane was discretized using a square mesh with a lattice constant of 1 nm and the background refractive index was set to 1.33. Perfectly matched boundary conditions were used in both directions. Dipole emission with a free space wavelength of $\lambda = 626$ nm was simulated. The dipoles were separated by one wavelength in the medium. Simulations were performed with the dipole oscillation axis along the vertical and the separation axis along the horizontal, and were then repeated with the dipole oscillation axis inclined 40° into the simulation plane. Analogous simulations were also performed for dipoles separated along a diagonal axis 30° from the horizontal. For the simulation with the dipole oscillation axis inclined and the dipoles separated along the diagonal, a phase angle between the emission from each dipole was introduced to model the delay between stimulation of adjacent scattering sites.

S4. Representative Fourier Spectra Fit Data

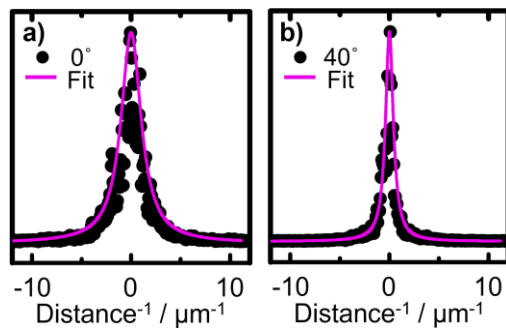


Figure S2. (a) and (b) Fourier spectrum and associated fit curve of the intensity along the vertical centerline of the positive fundamental mode in the 2D FT depicted in Figure 2a, and c, respectively.

S5. References

1. G. M. Hale and M. R. Querry, *Appl. Opt.*, 1973, **12**, 555-563.